THE JOURNAL OF BIOLOGICAL CHEMISTRY VOL. 284, NO. 19, pp. 12727–12734, May 8, 2009

Epigenetic Control of the Invasion-promoting MT1-MMP/MMP-2/TIMP-2 Axis in Cancer Cells*[S]

Received for publication, January 14, 2009, and in revised form, March 4, 2009 Published, JBC Papers in Press, March 13, 2009, DOI 10.1074/jbc.M900273200

Andrei V. Chernov, Nor Eddine Sounni, Albert G. Remacle, and Alex Y. Strongin[1]

From the Burnham Institute for Medical Research, La Jolla, California 92037

Membrane type-1 matrix metalloproteinase (MT1-MMP) is an activator of soluble MMP-2. The activity of both MMPs is regulated by their physiological inhibitor TIMP-2. An MT1-MMP/MMP-2/TIMP-2 axis plays a key role in the invasive behavior of many cell types. Despite its importance, epigenetic control of this pro-invasive axis is insufficiently studied, and, as a result, its modification in a rational and clinically beneficial manner is exceedingly difficult. Therefore, we performed an epigenetic analysis of the MT1-MMP, MMP-2, and TIMP-2 gene promoters in highly migratory glioblastoma cells and in low migratory breast carcinoma MCF-7 cells. We determined, for the first time, that the epigenetic control leading to the transcriptional silencing of both MMPs includes hypermethylation of the corresponding CpG regions and histone H3 lysine-27 trimethylation (H3K27me3). In turn, undermethylation of the CpG islands and low levels of histone H3 lysine-27 trimethylation are features of transcriptionally active MT1-MMP and MMP-2 genes in invasive cancer cells. Additional histone modifications we have analyzed, including H3ac and H3K4me2, are present in both transcriptionally active and inactive promoters of both MMPs. Histone H3 lysine-4 trimethylation is likely to play no significant role in regulating MT1-MMP and MMP-2. The pattern of epigenetic regulation of TIMP-2 was clearly distinct from that of MMPs and included the coordinated methylation and demethylation of the two CpG regions in the promoter. Our results suggest that the epigenetic control plays an important role in both the balanced regulation of the MT1-MMP/MMP-2/TIMP-2 axis and the invasive behavior in cancer cells.

Cleavage of the basement membrane and the extracellular matrix by cancer cell proteinases is a prerequisite for malignant cells to invade tissues and spread through the body (1). Matrix metalloproteinases (MMPs)[2] including MT1-MMP, play a highly significant and proved role in these processes (2, 3). MT1-MMP, a membrane proteinase with an extracellular catalytic domain and a short C-terminal cytoplasmic tail, is attached to the plasma membrane via a transmembrane domain. MT1-MMP is synthesized as an inactive precursor that is transformed into functionally active MT1-MMP by the cleavage action of furin-like proprotein convertases (4). MT1-MMP accumulates at the leading edge of the tumor cell and plays the most critical role in cell locomotion (5). MT1-MMP directly cleaves the extracellular matrix components and cell receptors and is the only activator of soluble MMP-2 (6). The activation of MMP-2 amplifies the aberrant proteolysis and facilitates the destruction of the matrix (7). TIMP-2 is a member of a multigene family (TIMP-1 through -4) that binds non-covalently to active MMPs in a 1:1 molar ratio and inhibits their activity (8). The equilibrium among MT1-MMP, MMP-2, and TIMP-2 is a major factor in the regulation of the proteolytic activity of both MMPs. The MT1-MMP/MMP-2 proteolytic cascade is closely linked to cancer metastases, progression, invasion, poor clinical stage, larger tumor size, and increasing tumor stage in cancer patients (9).

Gene products involved in cell locomotion, angiogenesis, tumor progression, and survival are all potential targets of epigenetic regulation via CpG methylation and histone modifications. In malignancies, DNA methylation is frequently disregulated. By interfering with the transcription initiation, methylation of the CpG sites inhibits transcription and represses tumor suppressor genes. Acetylation of the core histones H3, H4, H2A, and H2B are normally associated with the activation of gene transcription (10). Acetyl groups are added by a family of histone acetyl transferases (HATs) and are removed by histone deacetylases (HDACs).

In turn, methylation of the lysine residues in the histone tails leads to either transcriptional activation or repression methylation of histone lysines occurs as mono-, di-, and trimethylation (11) and is reversed by enzymatic demethylation (12). Methylation of residues H3K4, H3K36, and H3K79 attracts the polymerase II complex and up-regulates gene expression (13, 14). In contrast, methylation of lysines H3K9, H3K27, and H4K20 promotes the interaction of the modified histones with the heterochromatin protein 1 (HP1) or its homologues (15–18) and leads to gene silencing. H3K4 and H3K27 methylation frequently coexists in histones, which are associated with the temporarily silenced developmental genes, the rapid activation of which is initiated by the developmental stimuli (19, 20). In contrast to many other tumorigenic genes, it is still unclear if and how MT1-MMP, MMP-2, and TIMP are controlled epigenetically (21–24).

* This work was supported, in whole or in part, by National Institutes of Health Grants CA83017, CA77470, and RR020843. This work was also supported by Susan G. Komen Breast Cancer Foundation Grant BCTR123106 (to A. Y. S.).

[S] The on-line version of this article (available at http://www.jbc.org) contains supplemental Tables S1–S4.

[1] To whom correspondence should be addressed. E-mail: strongin@burnham.org.

[2] The abbreviations used are: MMP, matrix metalloproteinase; DMEM, Dulbecco's modified Eagle's medium; ChIP, chromatin immunoprecipitation; H3K4me2, dimethylated Lys-4 of histone H3; H3K4me3, trimethylated Lys-4 of histone H3; H3K27me3, trimethylated Lys-27 of histone H3; H3ac, pan-acetylated histone H3; MT1-MMP, membrane type-1 matrix metalloproteinase; MSP, methylation-sensitive PCR; TIMP-2, tissue inhibitor of matrix metalloproteinases-2.

Here, we determine, for the first time, the significance of epigenetic control including DNA methylation and histone modification, in the regulation of MT1-MMP, MMP-2, and TIMP-2. We now are confident that epigenetic regulation is a major player in the regulation of the MT1-MMP/MMP-2/TIMP-2 axis and, as a result, an important factor that controls tumor cell invasion and migration.

MATERIALS AND METHODS

Reagents—Reagents unless otherwise indicated were from Sigma. DNA oligonucleotides (supplemental Tables S1–S4) were synthesized by Eurogentec and Integrated DNA Technologies. Murine monoclonal antibodies against MT1-MMP (clone 3G4) and α-actin (clone C4), rabbit polyclonal anti-histone modification antibodies (H3K4me2, H3K4me3, and H3K27me3) and GM6001 (a hydroxamate inhibitor of MMPs) were purchased from Chemicon. A rabbit antibody against recombinant human H3 histone was from Cell Signaling Technologies. A goat polyclonal TIMP-2 antibody was purchased from R&D System. Recombinant TIMP-2 (rTIMP-2) was isolated from CHO cells stably transfected with the full-length human TIMP-2 cDNA gene.

Cell Cultures—Human fibrosarcoma HT1080, glioblastoma U251, U87, TP98G, and U373, and breast carcinoma MCF-7 were grown in DMEM supplemented with 10% fetal bovine serum (DMEM/FBS). 80–90% confluent cells were used in our experiments. U251 cells (U-MT/PDX cells) co-transfected with both MT1-MMP and α1-antitrypsin variant Portland (PDX), and MCF-7 cells stably transfected with the full-length MT1-MMP and the full-length β3 integrin subunit were isolated and characterized earlier (25, 26).

RT-PCR Analysis—Total RNA was isolated using a Mini RNA Isolation kit (Zymo Research). RT-PCR analysis (40 ng total RNA/reaction) was performed using a OneStep RT-PCR System (Qiagen) and the respective primers designed to amplify the genomic DNA (supplemental Table S1). RT-PCR reactions (35 cycles) were performed using denaturation at 95 °C for 30 s, annealing at 58 °C for 30 s and elongation at 72 °C for 1 min. The products were separated by gel electrophoresis.

In a large-scale RT-PCR analysis, cDNA was first synthesized using 1 μg of total RNA, 5 ng/μl random primers, and a SuperScript System (Invitrogen). The synthesized cDNA was next used as a template in the PCR reactions, which contained TaqDNA Polymerase (New England Biolabs), 0.4 mM dNTPs, and 0.6 μM primers.

Methylation-sensitive PCR (MSP)—The primers used in the MSP were designed using MethPrime software (27) (supplemental Table S2). PCR reactions (40 cycles) were performed using denaturation at 95 °C for 20 s, annealing at 53 °C for 20 s, and elongation at 72 °C for 20 s. Products were separated by gel electrophoresis.

Bisulfite DNA Sequencing—The bisulfite DNA conversion was performed using EZ DNA Methylation-Direct reagents (Zymo Research). Primers were designed using Primer 3 software (28) (supplemental Table S3). PCR products were cloned into the pCR2.1-TOPO vector using a TA TOPO Cloning kit (Invitrogen). The insert DNA fragments were amplified directly from the selected individual colonies using the 5′-ATTACGCCAGCTGGCGAAAGGGGGATGTG-3′ and 5′-CAGGCTTTACACTTTATGCTTCCGGCTCG-3′ oligonucleotides as the forward and reverse primers, respectively, and TaqDNA polymerase. The amplified PCR products were purified using a DNA Clean & Concentrator-5 (Zymo Research), and their nucleotide sequence was determined by DNA sequencing.

Chromatin Preparation—Cells (80% confluent) were treated with 1% paraformaldehyde for 10 min, then with sodium glycine (100 mM) to inactivate paraformaldehyde, washed twice with ice-cold phosphate-buffered saline and collected by centrifugation. Cells were resuspended in 20 mM Tris-HCl, pH 7.5, containing 150 mM NaCl, 3 mM $CaCl_2$, 0.2% Triton X-100, and the Complete Proteinase Inhibitor Mixture (Roche Applied Science). Chromatin DNA was digested at 37 °C for 10 min using micrococcal nuclease (Roche Applied Science) to generate ~80% mononucleosomal and 20% dinucleosomal DNA fragments. The reactions were stopped using 5 mM EDTA. Digested chromatin was solubilized for 15 min on ice using 0.2% SDS. The pellet was removed by centrifugation (10,000 × *g*, 20 min).

For each chromatin sample a corresponding control fraction of the input DNA was prepared as follows. Genomic DNA samples (50 μg each) were incubated for 16 h at 65 °C with 0.5 M NaCl. RNA and proteins were digested using 10 μg/ml RNase A (37 °C; 15 min) and 1 mg/ml proteinase K (50 °C; 1 h), respectively. DNA was purified using a PCR Purification system (Zymo Research). DNA concentration was measured at 260 nm.

Chromatin Immunoprecipitation (ChIP)—Chromatin samples (25–100 μg) were diluted in 500 μl of ChIP buffer (50 mM HEPES, pH 7.5, containing 150 mM NaCl, 0.5% Triton X-100, 1 mM EDTA, 0.1% sodium deoxycholate, 0.1% SDS, and the Complete Proteinase Inhibitor Mixture). The samples were precleared by incubating for 1 h at 4 °C with 50 μl of protein G-coated magnetic Dynabeads suspension (Invitrogen). The H3ac, H3K4me2, H3K4me3, or H3K27me3 antibodies (10 μg each) and 50 μl of protein G-coated magnetic Dynabeads suspension were then added to the precleared samples. Non-immune rabbit IgG was used as a control. To reduce nonspecific binding, the beads were pretreated for 1 h with the sonicated salmon sperm DNA (10 mg/ml). The final volume of the samples was made 600 μl using ChIP buffer. ChIP samples were prepared in triplicates. The samples that did not contain the antibody were used as controls. The samples were incubated at 4 °C for 12 h on a rotating platform. Beads were captured using a magnetic rack (Qiagen), washed four times in the ChIP buffer and twice in the ChIP buffer containing 0.5 M NaCl. The bound material was eluted from the beads at 37 °C for 30 min in 100 μl of 0.1% $NaHCO_3$, 1% SDS. The soluble fraction was separated from the beads by centrifugation (10,000 × *g*, 5 min). The soluble material was incubated 68 °C for 4 h in the presence of 0.5 M NaCl. RNA and proteins were digested using 10 μg/ml RNase A (37 °C; 15 min) and 0.25 mg/ml proteinase K (50 °C; 15 min), respectively. DNA was purified using a PCR purification kit. DNA concentration was measured at 260 nm.

Quantitative PCR Analysis of the Immunoprecipitated Chromatin—Reactions (25 μl each in triplicate) contained a Power SYBR green PCR mix (12.5 μl; Applied Biosystems), specific primers (10 pmol each), and DNA (2.5 ng). Primers (supplemental Table S4) were designed using Primer 3 software (28). Genomic DNA sequences were obtained from the NCBI data base (Human Genome Built 36.3). The PCR amplification was performed using an MX3000P thermocycler (Stratagene). ROX dye was used as an internal standard. Amplification was monitored by measuring a melting curve of the RT-PCR product. The amplified products were analyzed by gel electrophoresis. The data were processed by MxPro software (Stratagene) to calculate the Ct values of the RT-PCR products.

Treatment of Cells with 5-Aza-2′-deoxycytidine—Cells (1×10^5) were grown overnight in wells of a 6-well tissue plate. 5-Aza-2′-deoxycytidine (10 μM; Aza-dC) were then added to cells, and incubation was continued for an additional 3–7 days. The medium supplemented with Aza-dC was replaced every 12 h. After treatment, cells were kept overnight in the medium alone and were then analyzed.

Cell Migration—The efficiency of cell migration was measured in wells of a 24-well, 8-μm pore size Transwell plate (Costar). A 6.5-mm insert membrane was coated with 50 μl of type I collagen (100 μg/ml in DMEM) and then dried for 12 h. The collagen coating was re-hydrated in 0.5 ml of DMEM for 30 min immediately before the experiments. The inner chamber contained DMEM/FBS as chemoattractant. Cells (1×10^4) were seeded in the outer chamber in serum-free DMEM. GM6001 (10 μM) or DMSO alone (0.1%) were added to both inner and outer chambers 15 min prior to plating the cells. Cells were allowed to migrate for 12 h. Cells were removed from the upper membrane surface with a cotton swab. Cells that migrated to the membrane undersurface were stained with 0.2% Crystal Violet-20% methanol. The incorporated dye was extracted from cells using 0.25 ml 1% SDS. The A_{570} value of the extract was measured. Migrated cells were also counted in five random areas of the membrane using a light microscope. There was a high level of correlation between these two methods. Data are means ± S.E. from three individual experiments performed in triplicate. Statistical analysis was performed by the two-tailed unpaired *t* test. *p* values ≤0.05 were considered significant.

Cell Surface Biotinylation and Western Blotting of MT1-MMP—Cells (80–90% confluent) were washed with an ice-cold Soerensen buffer containing 14.7 mM KH_2PO_4, 2 mM Na_2HPO_4, pH 7.8, and 120 mM sorbitol and then incubated in this buffer for an additional 10 min. Cells were surface-biotinylated for 20 min on ice in Soerensen buffer containing 0.3 mg/ml membrane-impermeable EZ-Link NHS-LC-biotin (Thermo Scientific). The residual biotin was quenched for 10 min using 100 mM glycine. Cells were lysed in a modified radioimmune precipitation assay buffer (20 mM Tris-HCl, pH 7.4, 150 mM NaCl, 0.1% SDS, 1% sodium deoxycholate, 1% Nonidet P-40) supplemented with proteinase inhibitor mixture III (Calbiochem), 1 mM phenylmethylsulfonyl fluoride, and 10 mM EDTA. Biotin-labeled proteins were precipitated using streptavidin-agarose beads. The precipitates were analyzed by Western blotting with the MT1-MMP antibody followed by the goat secondary horseradish peroxidase-conjugated IgG (GE Healthcare) and a TMB/M substrate (Moss).

Gelatin Zymography—Cells (1×10^5) were grown in DMEM/fetal bovine serum in wells of a 48-well plate (Costar) until a 90% confluence. The medium was then replaced with DMEM. After incubation for 24 h, the medium samples were analyzed (25).

Western Blotting of TIMP—The levels of TIMP-2 were determined both in the medium and cell samples using Western blotting with a TIMP-2 antibody followed by donkey anti-goat IgG conjugated with horseradish peroxidase and a TMB/M substrate. rTIMP-2 was used as a control in Western blotting. Cells (2×10^6/10 cm dish) were grown 24 h in DMEM/10% fetal bovine serum. The medium was then replaced for DMEM (6 ml), and incubation was continued for an additional 24 h. Proteins from the medium samples were precipitated with 10% trichloroacetic acid on ice. The pellet was collected by centrifugation, washed with ice-cold acetone, dried, dissolved in 50 μl of 2× SDS reducing sample buffer and analyzed by Western blotting. The cells were lysed in a modified radioimmune precipitation assay buffer (20 mM Tris-HCl, pH 7.4, 150 mM NaCl, 0.1% SDS, 1% sodium deoxycholate, 1% Nonidet P-40) supplemented with proteinase inhibitor mixture III, 1 mM phenylmethylsulfonyl fluoride, and 10 mM EDTA. The lysate aliquots (20 μg of total protein each) were analyzed by Western blotting for TIMP-2. α-Actin was used as a loading control to assure equal loading among the samples.

RESULTS

Breast Carcinoma MCF-7 Cells Have Low Levels of Both MT1-MMP and MMP-2—We measured the migration efficiency of several cancer cell lines, which were derived from distinct tumor types. The selected cells lines included highly migratory fibrosarcoma HT1080 and glioblastoma (U251, U87, TP98G, and U373). We also used low-migratory breast carcinoma MCF-7 cells (29–34). As expected, we determined that only MCF-7 cells were incapable of efficient migration while other cell lines demonstrated a comparably high level of migration efficiency. In agreement, a potent, broad-range, hydroxamate inhibitor of MMPs, including MT1-MMP and MMP-2 efficiently inhibited migration of HT1080 cells but had no effect in MCF-7 cells (Fig. 1).

We next determined the levels of cell surface-associated MT1-MMP in biotin-labeled cells. To help us to identify the forms of MT1-MMP, we used U-MT/PDX cells as a reference. Because U-MT/PDX cells co-express MT1-MMP and PDX (an inhibitor of furin which is an MT1-MMP activator), they produced both the proenzyme and the enzyme of MT1-MMP (26). Using U-MT/PDX cells as a reference, we determined that the analyzed cells (except MCF-7) produced the activated, mature MT1-MMP enzyme (Fig. 2).

We used Western blotting of the medium and cell lysates to measure the levels of secretory and cell-associated TIMP-2. We also determined the activity of cellular MT1-MMP by assessing the activation status of MMP-2 using gelatin zymography of medium samples. According to these data, all of the cells except MCF-7 synthesized comparable levels of the active MT1-MMP enzyme, which were roughly equal to those in HT1080 cells. No

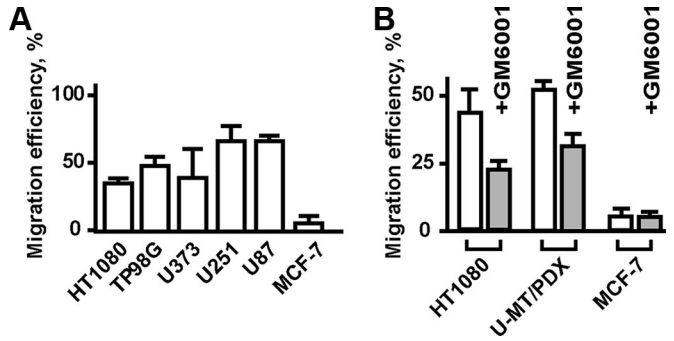

FIGURE 1. **Migration efficiency of cells.** *A*, cells (1×10^4) were allowed to migrate for 12 h in the wells of a Transwell plate using a membrane coated with type I collagen. *B*, an inhibitor of MMPs (GM6001) inhibits migration of HT1080 and U-MT/PDX cells. Where indicated, GM6001 (10 μM) was added to the cells. Migration efficiency was expressed as a percentage of the cells, which have migrated through the membrane and which were detected on the membrane undersurface relative to the total number of cells. The data are from three independent experiments performed in triplicate.

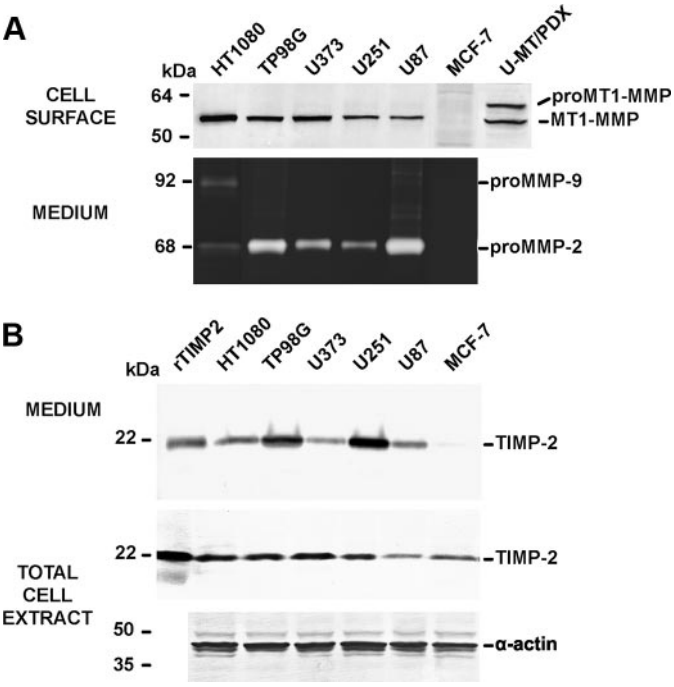

FIGURE 2. **MCF-7 cells synthesize TIMP-2 but not MT1-MMP and MMP-2.** *A*, Western blot analysis of cell surface-associated, biotin-labeled MT1-MMP (*top panel*) and gelatin zymography of secretory MMP-2 (*bottom panel*). U-MT/PDX cells which produce both the proenzyme and the enzyme of MT1-MMP were used as a reference in Western blots. *B*, Western blot analysis of secretory and cellular TIMP-2 (*top* and *middle panels*, respectively). rTIMP-2 was used as a reference. *Bottom panel*, Western blotting of cellular α-actin (loading control).

MT1-MMP was detected in MCF-7 cells. Similarly, all of the cells except MCF-7 produced the 68-kDa MMP-2 proenzyme (Fig. 2*A*). MMP-9 was detected in HT1080 and U87 cells. No MMP-2 and MMP-9 were detected in MCF-7 cells. The levels of cellular TIMP-2 were roughly similar among the tested cells including MCF-7. High levels of secreted TIMP-2 were detected in U251 and TP98G cells when compared with the other cell types (Fig. 2*B*).

In agreement, RT-PCR did not detect the mRNA of MMP-2 and MT1-MMP in MCF-7 cells while these mRNAs were readily amplified in the other cells. The levels of the TIMP-2 mRNA were similar in all cell lines including MCF-7 (Fig. 3*A*).

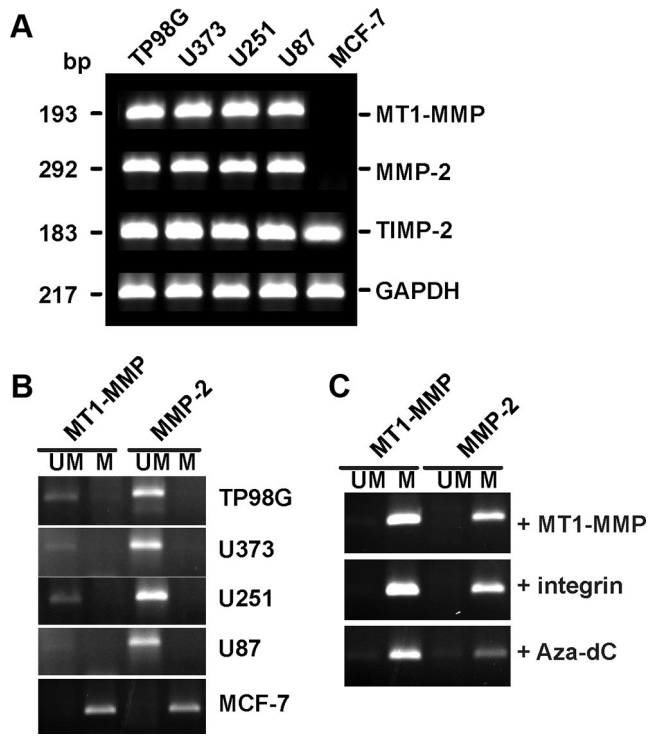

FIGURE 3. **MCF-7 cells do not express MT1-MMP and MMP-2 mRNA.** *A*, an RT-PCR analysis of the expression of the MT1-MMP, MMP-2, and TIMP-2 genes in TP98G, U373, U251, U87, and MCF-7 cells. The primers we used are shown in supplemental Table S1. The specific fragments of the expected size (193, 292, and 183 bp for MT1-MMP, MMP-2, and TIMP-2, respectively) were amplified. Glyceraldehyde-3-phosphate dehydrogenase (*GAPDH*) was used as a loading control. *B*, methylation-sensitive PCR of the MT1-MMP and MMP-2 promoter regions genes in TP98G, U373, U251, U87, and MCF-7 cells. UM and M, the PCR products are generated using the primers specific for unmethylated and methylated DNA, respectively. *C*, methylation-sensitive PCR of analysis of the MT1-MMP and MMP-2 promoter regions in MCF-7 cells stably transfected with the full-length MT1-MMP gene (+MT1-MMP) and the full-length β_3 integrin subunit (+*integrin*). The *bottom panel* shows the results of the analysis of untreated MCF-7 cells and MCF-7 cells subjected to demethylation using 5-aza-2′-deoxycytidine (+*Aza-dC*).

The Promoters of MT1-MMP and MMP-2 Are Hypermethylated in MCF-7 Cells—To determine if the epigenetic mechanisms silenced the synthesis of MT1-MMP and MMP-2 in MCF-7 cells, we determined the DNA methylation status of the MT1-MMP and MMP-2 gene promoters in the selected cell types. There is a 1.4-kb-long CpG island in the −0.1 to −1.3-kb region from the MT1-MMP transcription start site in the MT1-MMP promoter. This CpG island overlaps with the first exon of the MT1-MMP gene. A similar 1.0 kb-long CpG island is found in the −0.4 to −0.6 kb region relative to the MMP-2 transcription start site in the MMP-2 promoter. This region also overlaps with the first exon of the MMP-2 gene. The methylation status of these islands was determined using the primers, which were specific for the methylated (M) and unmethylated (UM) DNA in the bisulfite conversion-based PCR (Fig. 3*B*). We analyzed the 130–330 bp and 244–448 bp regions of the MT1-MMP and MMP-2 genes, respectively. (Numbering is provided relative to the transcription start site of the gene.) We determined that the genomic MT1-MMP and MMP-2 promoter regions were hypermethylated in MCF-7 cells. As a result, no undermethylated DNA was amplified in the PCR reactions. In contrast, the undermethylated DNA was predominantly

detected in the other cells, thus indicating low methylation levels of both MMP promoters in those cells distinct from MCF-7. The overexpression of MT1-MMP and integrin β3 did not affect the levels of hypermethylation of the genomic MT1-MMP locus in MCF-7 cells.

To induce demethylation, MCF-7 cells were co-incubated with Aza-dC (an inhibitor of DNA methylation) for several days. Aza-dC, induced a noticeable level of demethylation of MT1-MMP (Fig. 3*B*), which, as determined by Western blotting and gelatin zymography analyses, did not significantly increase the expression of MMP-2 and MT1-MMP (data not shown). Based on these results, we suspect that the epigenetic mechanisms additional to hypermethylation control the MT1-MMP and MMP-2 gene expression in MCF-7 cells.

To determine the methylation pattern in more detail, we analyzed the 240-bp-long sequence region (BIS region; 43–282 bp relative to the transcription start site) of the MT1-MMP promoter in MCF-7, TP98G, U373, U251, and U87 cells using the bisulfite sequencing of the amplified DNA fragments. These fragments included 15 CpG sites (Fig. 4). Similarly, bisulfite sequencing was used to determine the methylation status of 22 CpG sites of the 221-bp-long BIS1 region (228–448 bp from the transcription start site) and 6 CpG sites of the 230-bp-long BIS2 region (504–733 bp from the transcription start site) of the MMP-2 gene promoter in MCF-7 and U251 cells (Fig. 5). The data we obtained supported hypermethylation of both MMP genes in MCF-7 cells and undermethylation in the cells distinct from MCF-7. We conclude that methylation of the promoter sequence plays a significant role in regulating the transcriptional activity of MMPs and that hypermethylation resulted in a greatly reduced expression of MT1-MMP and MMP-2 in MCF-7 cells.

H3ac and H3K4me2 Epigenetic Marks in the MMP Genes—To determine if epigenetic mechanisms, additional to DNA methylation, are involved in the regulation of MT1-MMP and MMP-2, we determined the levels of histone modification in the promoter regions of these MMPs. We specifically selected to measure the H3K27me3, H3K4me2, H3K4me3, and pan-acetyl histone H3 modifications because the levels of these epigenetic marks vary significantly among the transcriptionally silenced and the transcriptionally active genes (35, 36).

We used six primer pairs (Fig. 4*A*, *primers A1–A6*) from a 4.1-kb-long region of the MT1-MMP promoter (−1.4 to −2.7 kb relative to the MT1-MMP transcription start site). Similarly, five primer pairs (Fig. 5*A*, *primers B1–B5*) were used to analyze a 3-kb-long region of the MMP-2 promoter (−0.7 to −2.3 kb relative to the MMP-2 transcription start site). As a control, we determined the levels of histone modifications in the transcriptionally active ribosomal protein L30 (RPL30). Quantitative real-time PCR was performed using the ChIP samples as templates. The samples were analyzed in triplicate using at least three independent ChIP experiments. To quantitatively assess the levels of the immunoprecipitated chromatin, we calculated the mean PCR amplification-threshold values (Ct values) for each ChIP sample. The mean Ct values were normalized against the Ct values of the non-immune rabbit IgG control. The data of the representative ChIP experiments are shown in Figs. 4 and 5.

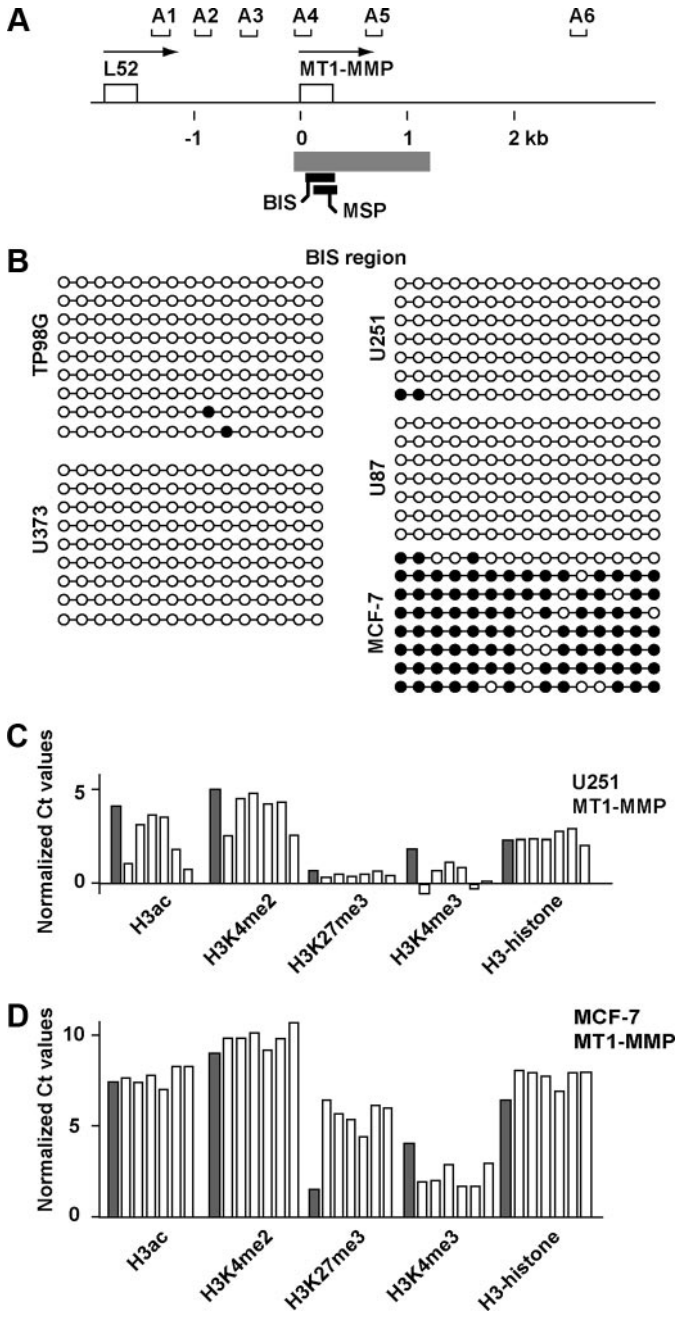

FIGURE 4. **Epigenetic analysis of the MT1-MMP gene in cancer cells.** *A*, schematic presentation of the human MT1-MMP promoter region. The upstream L52 gene is on the *left*. The first exon is shown as an *open box*. The *arrows* show the transcription start sites. The *gray box* indicates the 1.4-kb-long CpG island. *Black boxes* show the regions that were analyzed using the bisulfite sequencing (*BIS*) and MSP. The A1–A6 regions were analyzed using ChIP. *B*, the bisulfite sequencing of the 240-bp-long BIS fragment containing 15 CpG islands in TP98G, U373, U251, U87, and MCF-7 cells. The methylation status of each CpG dinucleotide was determined by sequencing of at least seven independent PCR clones of bisulfite-converted DNA. The primers we used are shown in supplemental Table S3. Each *circle* represents an individual CpG. *Open* and *closed circles* indicate unmethylated and methylated CpGs, respectively. *C* and *D*, ChIP analysis of the MT1-MMP promoter region in U251 and MCF-7 cells, respectively. *Gray bars*, the Ct values of the transcriptionally active RLP30 control gene. *Open bars*, the Ct values which correspond to the A1–A6 primer pairs in the order shown in *A*. H3ac, H3K4me2, H3K27me3, and H3K4me3 represent the analyzed histone modifications. Total H3 histone ChIP was used as an additional control.

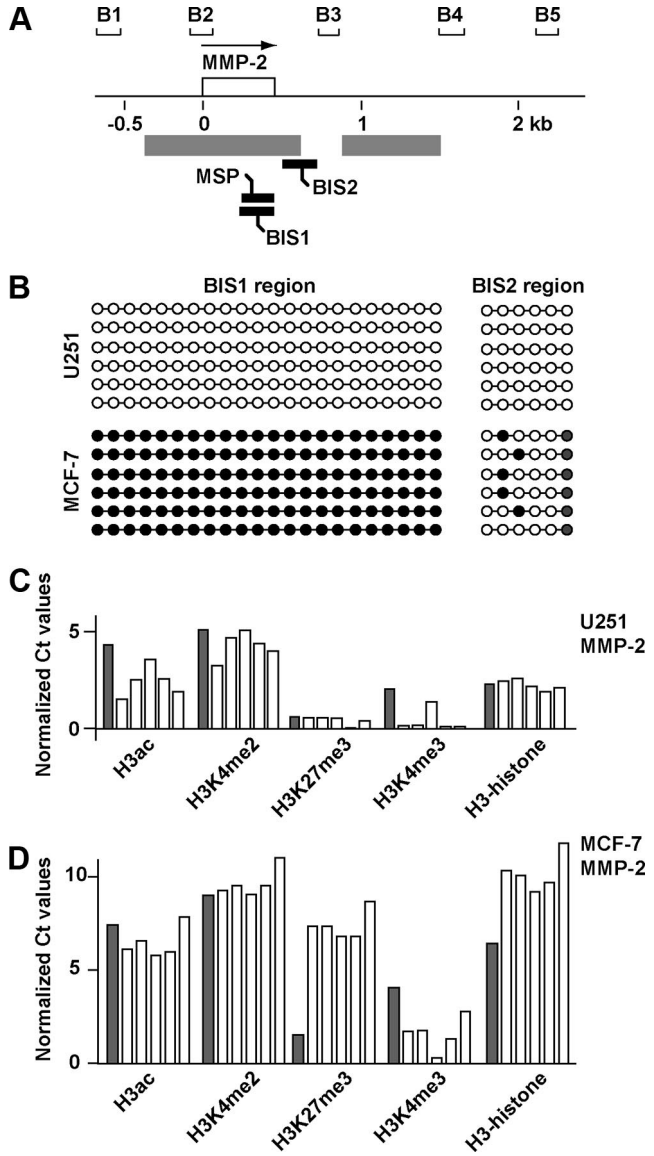

FIGURE 5. **Epigenetic analysis of the MMP-2 gene in cancer cells.** *A*, schematic presentation of the human MMP-2 promoter region. The first exon is shown as an *open box*. The *arrow* shows the transcription start site. The *gray boxes* indicate the two CpG-rich regions. *Black boxes* show the regions that were analyzed using the bisulfite sequencing (*BIS1* and *BIS2*) and MSP. The B1–B5 regions were analyzed using ChIP. *B*, bisulfite sequencing of the 221-bp-long BIS1 fragment with 22 CpG islands and the 230-bp-long BIS2 fragment with 6 CpG islands in U251 and MCF-7 cells. The methylation status of each CpG dinucleotide was determined by sequencing at least six independent PCR clones of bisulfite-converted DNA. The primers we used are shown in supplemental Table S3. Each *circle* represents an individual CpG. *Open* and *closed circles* indicate unmethylated and methylated CpGs, respectively. *C* and *D*, ChIP analysis of the MMP-2 promoter region in U251 and MCF-7 cells, respectively. *Gray bars*, the Ct values of the transcriptionally active RLP30 control gene. *Open bars*, the Ct values which correspond to the B1-B5 primer pairs in the order shown in *A*. H3ac, H3K4me2, H3K27me3, and H3K4me3 represent the analyzed histone modifications. Total H3 histone ChIP was used as an additional control.

The ChIP samples of the transcriptionally active MMP-2 and MT1-MMP genes of U251 cells exhibited high levels of the H3ac and H3K4me2 histone modifications. In the transcriptionally silent MMP-2 and MT1-MMP genes in MCF-7 cells, the levels of H3ac and H3K4me2 epigenetic marks were also high. Surprisingly, the level of the H3K4me3 histone modification, which is normally a hallmark of active human promoters (37), was not dramatically higher in the transcriptionally active MMP-2 and MT1-MMP genes in U251 cells when compared with MCF-7 cells suggesting that H3K4me3 does not play a role in the regulation of these MMP genes.

The level of the H3K27me3 modification was high in the transcriptionally silent MMP genes in MCF-7 cells, especially when compared with that of the RPL30 gene. Conversely, the level of the H3K27me3 mark was low in both transcriptionally active MMP genes in U251 cells. Overall, the levels of histone modification marks in the transcriptionally active MMP genes in U251 cells correlated well with those of the RPL30 gene control. Because H3K27me3 is a consistent histone modification that marks the inactive genomic loci, our results suggest that H3K27me3 together with DNA hypermethylation resulted in the transcriptional silencing of the MMP-2 and MT1-MMP gene in MCF-7 cells.

Specific Patterns of CpG Island Methylation of the Transcriptionally Active TIMP-2 Gene—To establish if epigenetic regulation of TIMP-2 correlates with that of MMP-2 and MT1-MMP, we determined the DNA methylation status of the TIMP-2 gene promoter in TP98G, U373, U251, U87, and MCF-7 cells. There is a well-defined 1.35-kb-long CpG island in the promoter of the TIMP-2 gene. This island is localized in the −0.5 to −0.85 kb region relative to the transcription start site. Hypermethylation of this island was previously reported to result in lost expression of the TIMP-2 gene in human prostate tumors (23). There is, however, an additional, previously unidentified 0.5-kb-long CpG island in the TIMP-2 gene. We determined that this 0.5-kb-long island is localized in the −1.7 to −1.2 kb region relative to the TIMP-2 transcription start site. To identify the methylation status of the 0.5-kb-long and 1.35-kb-long CpG islands we used the primers derived from the BIS1 and BIS2 regions (−1679 to −1350 bp and −581 to −361 bp from the transcription start site, respectively). The bisulfite sequencing was used to analyze 16 and 12 CpG sites of the 329-bp-long BIS1 and 220-bp-long BIS2 regions, respectively (Fig. 6). The 1.35-kb-long CpG island was not extensively methylated in the cells we analyzed. In turn, there was hypermethylation of the 0.5-kb-long CpG island suggesting that the methylation ratio of these two islands plays a role in regulating TIMP-2 and that the epigenetic regulation of TIMP-2 in cancer is clearly distinct from that of MMP-2 and MT1-MMP.

DISCUSSION

Cell surface-associated MT1-MMP and soluble-secreted MMP-2 (a target of MT1-MMP activation), and their inhibitor TIMP-2 have been extensively studied as proteins (2, 7). TIMP-2 plays an essential role both in the inhibition of the proteolytic activity of both MMPs, and in the activation of MMP-2 by MT1-MMP. In the process of MMP-2 activation, TIMP-2 binds cell surface MT1-MMP. The bi-molecular MT1-MMP·TIMP-2 complex then binds the proenzyme of MMP-2 and initiates the activation cascade leading to the release of the active MMP-2 enzyme into the extracellular milieu (38). If MT1-MMP is inactivated, MMP-2 remains a latent zymogen. As a result, MT1-MMP and MMP-2 are closely interconnected. MMP-2 knock-out has an insignificant effect in mice (39). In sharp contrast, MT1-MMP knock-out mice are dwarfs with

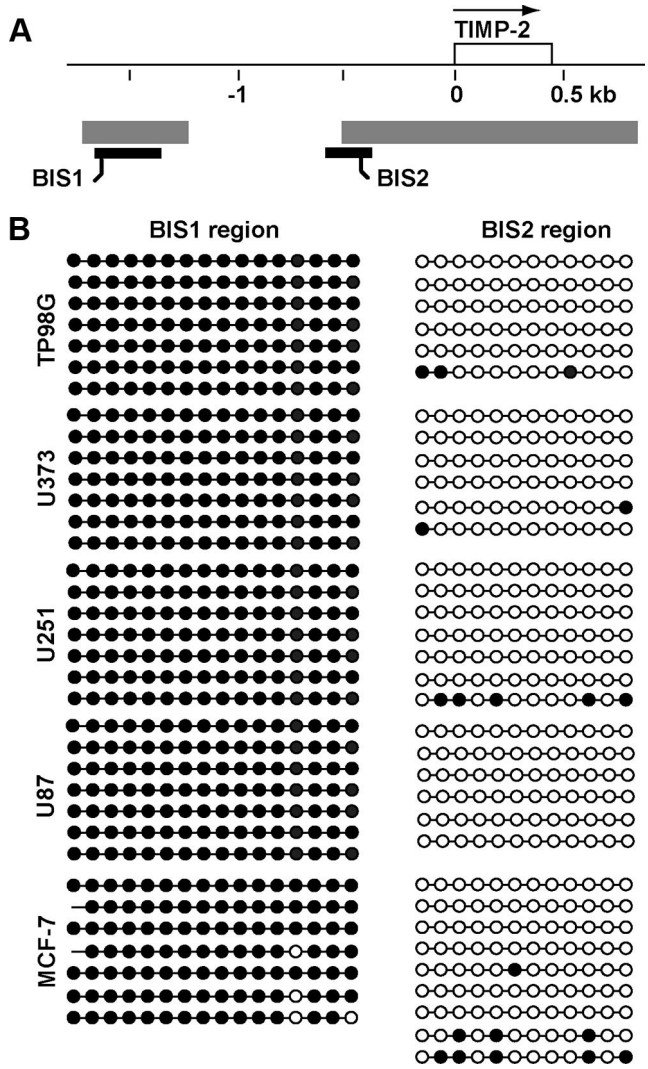

FIGURE 6. **Epigenetic analysis of the TIMP-2 gene in cancer cells.** *A*, schematic presentation of the human TIMP-2 promoter region. The first exon is shown as an *open box*. The *arrow* shows the transcription start site. The *gray boxes* indicate the two CpG-rich regions, which are localized 1.7-kb and 0.5-kb upstream of the transcription start site. *Black boxes* show the regions which were analyzed using the bisulfite sequencing (*BIS1* and *BIS2*). *B*, the bisulfite sequencing of the 329-bp-long BIS1 fragment with 16 CpG islands and the 220-bp-long BIS2 fragment with 12 CpG islands in TP98G, U373, U251, U87, and MCF-7 cells. The methylation status of each CpG dinucleotide was determined by sequencing of at least six independent PCR clones of bisulfite-converted DNA. The primers we used are shown in supplemental Table S3. Each *circle* represents an individual CpG. *Open* and *closed circles* indicate unmethylated and methylated CpGs, respectively.

craniofacial dysmorphism, arthritis, osteopenia, and fibrosis of soft tissues (40). Mice lacking both MMP-2 and MT1-MMP, however, die immediately after birth with respiratory failure, abnormal blood vessels, and immature muscle fibers reminiscent of central core disease (41) thus suggesting the critical functional importance of the MT1-MMP/MMP-2 axis.

The MT1-MMP/MMP-2/TIMP-2 axis plays a key role in the invasive behavior of many cell types. Despite its obvious importance, epigenetic control of this pro-invasive axis is insufficiently studied and, as a result, its modification in a rational and clinically beneficial manner is exceedingly difficult. To fill this gap in our knowledge, we performed an epigenetic analysis of the gene promoters of MT1-MMP, MMP-2, and TIMP-2 in highly migratory glioblastoma cells and in low migratory breast carcinoma MCF-7 cells. We determined that the similar, strict, and redundant, epigenetic regulation of both MMPs is coordinately regulated by DNA methylation and by histone modifications. The deposition of H3K27me3 histone and hypermethylation of the CpG islands overlapping with the MMP-2 and MT1-MMP gene promoters is a characteristic of the transcriptionally inactive MMP-2 and MT1-MMP genes in MCF-7 cells. In contrast, undermethylation and a low level of histone H3 trimethylation including H3K4me3 and especially H3K27me3 is a characteristic pattern of the proteinase promoters in the invasive, migratory cancer cells. Additional histone modifications we have analyzed, including H3ac and H3K4me2, are present in both transcriptionally active and inactive promoters of both MMPs. It should be noted that in human embryonic stem cells silent developmental gene loci frequently include the repressive H3K27 methylation marks (42, 43). At the same time, H3K4 methylation that is normally a feature of transcriptionally active chromatin, is also present in these loci, probably, serving as a predisposition for the subsequent rapid activation and gene expression (19, 20). Consequently, it is likely that the presence of the H3K4me2 mark in the MMP genes in MCF-7 cells suggests that these genes can be rapidly activated in cancer cells, when required.

The presence of high levels of the repressive H3K27me3 epigenetic mark explains why DNA demethylation alone was insufficient to induce the transcriptional activation of the MMP-2 and MT1-MMP promoters in Aza-dC-treated MCF-7 cells. This redundant and multilayer epigenetic regulation of MMP-2 and MT1-MMP may contribute to the low efficacy of the specific inhibitors of histone deacetylases (HDACs) and histone acetylases (HATs) in cancer (44).

The pattern of epigenetic regulation of TIMP-2 was clearly distinct from that of the two MMPs. In addition to the previously known, 1.35-kb-long, CpG island that spans the transcription initiation start site of the TIMP-2 gene, we identified the other, 0.5-kb-long, CpG region that is localized upstream of the gene transcription site. While the 1.35-kb-island was largely undermethylated, the 0.5-kb-long island was hypermethylated in all of the cancer cell type we analyzed. We suspect that the hypermethylated 0.5-kb-long CpG island serves as a negative regulator of TIMP-2 and harbors the recognition sites for the methylation-sensitive repression factors (45).

Our findings of the multiple modes of cell line-specific and, potentially, tumor type-specific epigenetic regulation of MMPs present a challenge for the design of the therapeutic inhibitors. The effective cancer treatment should include several inhibitors targeting these redundant epigenetic mechanisms, including DNA methylation and histone acetylation and methylation, which, unfortunately, exist in cancer patients. We believe that successful treatment strategy requires the extensive epigenetic profiling of the individual cancer patients.

In summary, we conclude that MT1-MMP, MMP-2, and TIMP-2 are regulated in a coordinated and complex, albeit distinct, manner by a variety of epigenetic factors. Our observations suggest that DNA hypermethylation of the promoter region and the histone modification H3K27me3 are the key factors, which repress the transcriptional efficiency of the

MMP-2 and MT1-MMP genes. In turn, undermethylation and low levels of H3K27me3 correlate with the transcriptional activity of the MMP-2 and MT1-MMP genes. Epigenetic regulation of TIMP-2 is distinct from MMPs and includes the coordinated methylation and demethylation of the two CpG regions in the gene promoter.

REFERENCES

1. Friedl, P., and Wolf, K. (2008) *Cancer Res.* **68,** 7247–7249
2. Egeblad, M., and Werb, Z. (2002) *Nat. Rev. Cancer* **2,** 161–174
3. Itoh, Y. (2006) *IUBMB Life* **58,** 589–596
4. Seidah, N. G., Mayer, G., Zaid, A., Rousselet, E., Nassoury, N., Poirier, S., Essalmani, R., and Prat, A. (2008) *Int. J. Biochem. Cell Biol.* **40,** 1111–1125
5. Osenkowski, P., Toth, M., and Fridman, R. (2004) *J. Cell. Physiol.* **200,** 2–10
6. Strongin, A. Y. (2006) *Cancer Metastasis Rev.* **25,** 87–98
7. Murphy, G., Stanton, H., Cowell, S., Butler, G., Knauper, V., Atkinson, S., and Gavrilovic, J. (1999) *APMIS* **107,** 38–44
8. Clark, I. M., Swingler, T. E., Sampieri, C. L., and Edwards, D. R. (2008) *Int. J. Biochem. Cell Biol.* **40,** 1362–1378
9. Noel, A., Maillard, C., Rocks, N., Jost, M., Chabottaux, V., Sounni, N. E., Maquoi, E., Cataldo, D., and Foidart, J. M. (2004) *J. Clin. Pathol.* **57,** 577–584
10. Fry, C. J., and Peterson, C. L. (2001) *Curr. Biol.* **11,** R185–197
11. Turner, B. M. (2005) *Nat. Struct. Mol. Biol.* **12,** 110–112
12. Swigut, T., and Wysocka, J. (2007) *Cell* **131,** 29–32
13. Zhang, Y., and Reinberg, D. (2001) *Genes Dev.* **15,** 2343–2360
14. Kouzarides, T. (2007) *Cell* **128,** 693–705
15. Bannister, A. J., Zegerman, P., Partridge, J. F., Miska, E. A., Thomas, J. O., Allshire, R. C., and Kouzarides, T. (2001) *Nature* **410,** 120–124
16. Lachner, M., O'Carroll, D., Rea, S., Mechtler, K., and Jenuwein, T. (2001) *Nature* **410,** 116–120
17. Nakayama, J., Rice, J. C., Strahl, B. D., Allis, C. D., and Grewal, S. I. (2001) *Science* **292,** 110–113
18. Peters, A. H., Mermoud, J. E., O'Carroll, D., Pagani, M., Schweizer, D., Brockdorff, N., and Jenuwein, T. (2002) *Nat. Genet.* **30,** 77–80
19. Azuara, V., Perry, P., Sauer, S., Spivakov, M., Jorgensen, H. F., John, R. M., Gouti, M., Casanova, M., Warnes, G., Merkenschlager, M., and Fisher, A. G. (2006) *Nat. Cell Biol.* **8,** 532–538
20. Bernstein, B. E., Mikkelsen, T. S., Xie, X., Kamal, M., Huebert, D. J., Cuff, J., Fry, B., Meissner, A., Wernig, M., Plath, K., Jaenisch, R., Wagschal, A., Feil, R., Schreiber, S. L., and Lander, E. S. (2006) *Cell* **125,** 315–326
21. Chicoine, E., Esteve, P. O., Robledo, O., Van Themsche, C., Potworowski, E. F., and St-Pierre, Y. (2002) *Biochem. Biophys. Res. Commun.* **297,** 765–772
22. Clark, I. M., Swingler, T. E., and Young, D. A. (2007) *Front. Biosci.* **12,** 528–535
23. Pulukuri, S. M., Patibandla, S., Patel, J., Estes, N., and Rao, J. S. (2007) *Oncogene* **26,** 5229–5237
24. Roach, H. I., Yamada, N., Cheung, K. S., Tilley, S., Clarke, N. M., Oreffo, R. O., Kokubun, S., and Bronner, F. (2005) *Arthritis Rheum.* **52,** 3110–3124
25. Deryugina, E. I., Bourdon, M. A., Luo, G. X., Reisfeld, R. A., and Strongin, A. (1997) *J. Cell Sci.* **110,** 2473–2482
26. Golubkov, V. S., Chekanov, A. V., Doxsey, S. J., and Strongin, A. Y. (2005) *J. Biol. Chem.* **280,** 42237–42241
27. Li, L. C., and Dahiya, R. (2002) *Bioinformatics* **18,** 1427–1431
28. Rozen, S., and Skaletsky, H. (2000) *Methods Mol. Biol.* **132,** 365–386
29. Abd El-Aziz, S. H., Endo, Y., Miyamaori, H., Takino, T., and Sato, H. (2007) *Cancer Sci.* **98,** 1330–1335
30. Atkinson, S. J., Roghi, C., and Murphy, G. (2006) *Biochem. J.* **398,** 15–22
31. Deryugina, E. I., Ratnikov, B. I., Postnova, T. I., Rozanov, D. V., and Strongin, A. Y. (2002) *J. Biol. Chem.* **277,** 9749–9756
32. Ratnikov, B. I., Rozanov, D. V., Postnova, T. I., Baciu, P. G., Zhang, H., DiScipio, R. G., Chestukhina, G. G., Smith, J. W., Deryugina, E. I., and Strongin, A. Y. (2002) *J. Biol. Chem.* **277,** 7377–7385
33. Rozanov, D. V., Deryugina, E. I., Ratnikov, B. I., Monosov, E. Z., Marchenko, G. N., Quigley, J. P., and Strongin, A. Y. (2001) *J. Biol. Chem.* **276,** 25705–25714
34. Sounni, N. E., Roghi, C., Chabottaux, V., Janssen, M., Munaut, C., Maquoi, E., Galvez, B. G., Gilles, C., Frankenne, F., Murphy, G., Foidart, J. M., and Noel, A. (2004) *J. Biol. Chem.* **279,** 13564–13574
35. Barski, A., Cuddapah, S., Cui, K., Roh, T. Y., Schones, D. E., Wang, Z., Wei, G., Chepelev, I., and Zhao, K. (2007) *Cell* **129,** 823–837
36. Zhao, X. D., Han, X., Chew, J. L., Liu, J., Chiu, K. P., Choo, A., Orlov, Y. L., Sung, W. K., Shahab, A., Kuznetsov, V. A., Bourque, G., Oh, S., Ruan, Y., Ng, H. H., and Wei, C. L. (2007) *Cell Stem Cell* **1,** 286–298
37. Bernstein, B. E., Humphrey, E. L., Erlich, R. L., Schneider, R., Bouman, P., Liu, J. S., Kouzarides, T., and Schreiber, S. L. (2002) *Proc. Natl. Acad. Sci. U. S. A.* **99,** 8695–8700
38. Strongin, A. Y., Collier, I., Bannikov, G., Marmer, B. L., Grant, G. A., and Goldberg, G. I. (1995) *J. Biol. Chem.* **270,** 5331–5338
39. Itoh, T., Ikeda, T., Gomi, H., Nakao, S., Suzuki, T., and Itohara, S. (1997) *J. Biol. Chem.* **272,** 22389–22392
40. Holmbeck, K., Bianco, P., Caterina, J., Yamada, S., Kromer, M., Kuznetsov, S. A., Mankani, M., Robey, P. G., Poole, A. R., Pidoux, I., Ward, J. M., and Birkedal-Hansen, H. (1999) *Cell* **99,** 81–92
41. Oh, J., Takahashi, R., Adachi, E., Kondo, S., Kuratomi, S., Noma, A., Alexander, D. B., Motoda, H., Okada, A., Seiki, M., Itoh, T., Itohara, S., Takahashi, C., and Noda, M. (2004) *Oncogene* **23,** 5041–5048
42. Boyer, L. A., Plath, K., Zeitlinger, J., Brambrink, T., Medeiros, L. A., Lee, T. I., Levine, S. S., Wernig, M., Tajonar, A., Ray, M. K., Bell, G. W., Otte, A. P., Vidal, M., Gifford, D. K., Young, R. A., and Jaenisch, R. (2006) *Nature* **441,** 349–353
43. Lee, T. I., Jenner, R. G., Boyer, L. A., Guenther, M. G., Levine, S. S., Kumar, R. M., Chevalier, B., Johnstone, S. E., Cole, M. F., Isono, K., Koseki, H., Fuchikami, T., Abe, K., Murray, H. L., Zucker, J. P., Yuan, B., Bell, G. W., Herbolsheimer, E., Hannett, N. M., Sun, K., Odom, D. T., Otte, A. P., Volkert, T. L., Bartel, D. P., Melton, D. A., Gifford, D. K., Jaenisch, R., and Young, R. A. (2006) *Cell* **125,** 301–313
44. Curtin, M., and Glaser, K. (2003) *Curr. Med. Chem.* **10,** 2373–2392
45. Ohlsson, R., Renkawitz, R., and Lobanenkov, V. (2001) *Trends Genet.* **17,** 520–527